

https://doi.org/10.1130/G50982.1

Manuscript received 2 December 2022 Revised manuscript received 22 February 2023 Manuscript accepted 25 February 2023

Published online 19 April 2023

© 2023 Geological Society of America. For permission to copy, contact editing@geosociety.org

Making sense of shear zone fabrics that record multiple episodes of deformation: Electron backscatter diffraction-derived and crystallographic vorticity axis-enhanced petrochronology

Elena A. Miranda^{1,*}, Virginia Brown¹, Joshua J. Schwartz¹, and Keith A. Klepeis²

¹Department of Geological Sciences, California State University Northridge, 18111 Nordhoff Street, Northridge, California 91330-8266, USA

²Department of Geography and Earth Sciences, University of Vermont, 94 University Place, Burlington, Vermont 05405-0114, USA

ABSTRACT

We present a new method of linking microstructures, electron backscatter diffraction (EBSD)-derived crystallographic vorticity axis (CVA) analysis, and titanite petrochronology to directly link fabric development to specific deformation events in shear zone rocks with complex histories. This approach is particularly useful where overprinting is incomplete, such that it is unknown which fabric is being dated by the petrochronometer. Here, we compared single-phase CVA patterns of fabric-forming minerals with those of synkinematic petrochronometers (e.g., titanite) to associate the timing of fabric development with deformational events in the middle crust of the George Sound shear zone, Fiordland, New Zealand. The host rocks to the George Sound shear zone include the Carboniferous Large Pluton, where titanite petrochronology demonstrates an unequivocally Cretaceous age of metamorphic titanite growth within mylonitic foliation. However, the host rocks show two distinct CVA patterns: a transfensional deformation event recorded by quartz and plagioclase, and a pure-shear-dominated transpressional deformation event recorded by biotite and titanite. Therefore, the transpressional CVA pattern of the titanite, coupled with its Cretaceous age, shows that it cannot be used to date the quartz and plagioclase fabric developed in response to an older transtensional deformation event. These results demonstrate the necessity of combining EBSD and CVA analysis with petrochronology to demonstrate that synkinematic accessory phase petrochronometers show the same kinematic deformation geometry (i.e., CVA pattern) as the fabric being dated.

INTRODUCTION

Determining the evolution of faults and shear zones is essential for reconstructing the tectonic history of deformed regions (e.g., Lister and Williams, 1979). One key component of determining this history is the ability to directly date shear zone deformation (e.g., Oriolo et al., 2018). However, this is especially problematic in regions that have experienced multiple deformation events because most fabric-forming minerals such as quartz and plagioclase cannot be directly dated. One way around this is to use petrochronology of accessory phases as a proxy to date fabric development in high-temperature (450–750 °C) shear zone rocks (Buriticá et al., 2019; Moser

Elena Miranda **b** https://orcid.org/0000-0001

et al., 2022; Odlum et al., 2022). The fundamental premise of this approach is that the petrochronometer grows and/or deforms during deformation such that dating the accessory phases also dates the fabric. Therefore, it is implicitly assumed that the fabric-forming minerals and the petrochronometers deform and/or form together, which may be problematic in the absence of data that explicitly link the crystal-plastic deformation of the petrochronometer and the fabric to demonstrate a shared geometry of flow. This assumption can be problematic in shear zones with complex histories, where relict deformation fabrics may be partially overprinted, and where it is unclear which fabric development event is recorded by the accessory mineral being used as the petrochronometer (e.g., titanite, apatite).

One solution to this problem is to link the kinematic deformation geometry of host and

accessory minerals in a shear zone through crystallographic vorticity axis (CVA) analysis using electron backscatter diffraction (EBSD) techniques (Michels et al., 2015). Shear zone vorticity provides constraints on the kinematics of deformation, where the magnitude of spin about a vorticity vector is used to infer relative amounts of progressive pure shear and simple shear (Means et al., 1980; Tikoff and Fossen, 1995; Giorgis et al., 2017). In CVA analysis, a vorticity axis is calculated from the lattice distortion of minerals that have undergone hightemperature crystal-plastic deformation during shear zone fabric development. The orientation of the vorticity axis relative to the deformation fabric elements (i.e., foliation and lineation) defines the kinematic deformation geometry, and it is used to infer tectonic regimes (e.g., transtension, transpression, etc.) (Michels et al., 2015; Giorgis et al., 2017; Kruckenberg et al., 2019; Piette-Lauzière et al., 2020). The vorticity axes of individual minerals, including accessory mineral petrochronometers, can be extracted to evaluate how individual fabric elements record the tectonic regime. It is this aspect that uniquely renders CVA analysis as a necessary tool for demonstrating that petrochronometers share the same kinematic deformation geometry as that recorded in the fabric-forming minerals. Here, we used EBSD-derived CVA analyses and titanite petrochronology to reveal the preservation of a cryptic, regional Carboniferous transtensional tectonic event that was partially overprinted by a Cretaceous transpressional tectonic event within a reactivated shear zone. In the absence of CVA data, the two tectonic events would not be distinguishable; thus, our data show how CVA-coupled petrochronology can document the temporal and kinematic evolution of complex shear zones.

CITATION: Miranda, E.A., et al., 2023, Making sense of shear zone fabrics that record multiple episodes of deformation: Electron backscatter diffraction–derived and crystallographic vorticity axis–enhanced petrochronology: Geology, v. XX, p. https://doi.org/10.1130/G50982.1

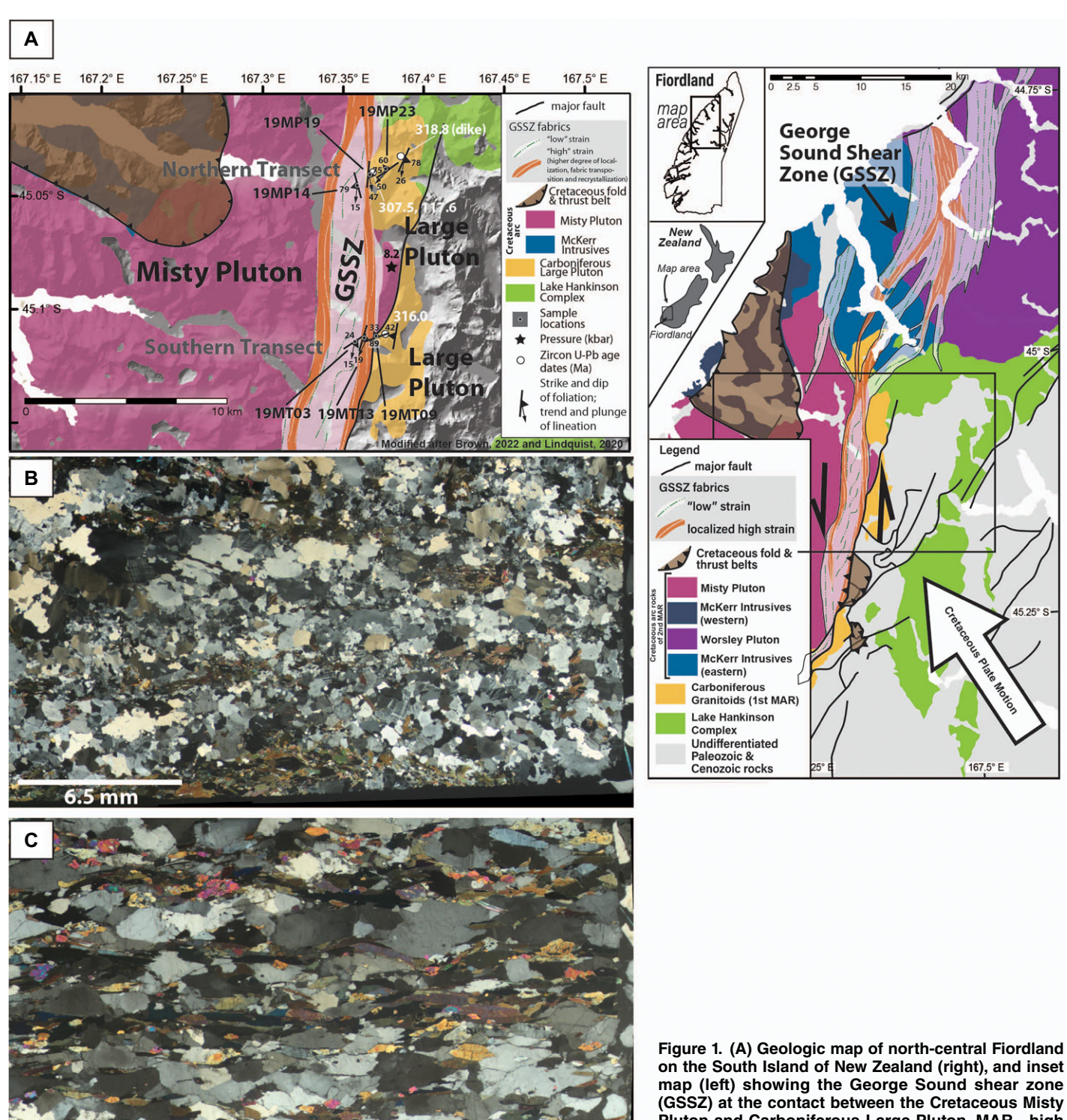
^{*}elena.miranda@csun.edu

GEOLOGICAL SETTING, SAMPLES, AND METHODS

The Zealandia Cordillera records \sim 400 m.y. of nearly continuous subduction-related arc magmatism that was punctuated by two events with a high magma addition rate (MAR) in the Devonian–Carboniferous (370–305 Ma) and the Cretaceous (129–105 Ma) (Ringwood et al.,

2021). The lower to middle crust of the arc is exposed in Fiordland, New Zealand (Fig. 1), where a system of Early Cretaceous intra-arc shear zones is developed within the arc rocks (Klepeis et al., 2022). The George Sound shear zone (GSSZ) is one of the largest Early Cretaceous intra-arc shear zones in Fiordland, and it developed along a preexisting crustal-scale

discontinuity that was a locus of pluton emplacement for both high-MAR events (Klepeis et al., 2019, 2022). In the middle crust, the GSSZ is the contact between the Carboniferous Large Pluton, emplaced during the first MAR event, and the Cretaceous Misty Pluton, emplaced during the second MAR event (Fig. 1). There, the GSSZ is \sim 3–5 km wide, and mylonitic fabrics



(GSSZ) at the contact between the Cretaceous Misty Pluton and Carboniferous Large Pluton. MAR—high magma addition rate. (B) Photomicrograph of Large Pluton sample 19MP19. (C) Photomicrograph of Misty Pluton sample 19MT13.

are developed within both the Misty Pluton and the Large Pluton; mylonitic fabrics are also observed within the Large Pluton outside of the GSSZ.

U-Pb zircon ages from the Large Pluton and from the Misty Pluton range 316–308 Ma and 117–114 Ma, respectively (Klepeis et al., 2022). Al-in-hornblende barometry in the Misty Pluton indicates crystallization at pressures of 8.2 kbar, consistent with middle-crustal depths (Greenberg, 2022). The GSSZ formed at the end of Misty Pluton emplacement (ca. 112 Ma) and at temperatures of ~700°C, based on Zr-in-titanite thermometry of metamorphic titanites in mylonitic fabrics within the Large Pluton (Brown, 2022; Klepeis et al., 2022).

We chose samples for EBSD + CVA analyses across the strain gradient of the GSSZ along two transects (Fig. 1A, inset). The northern transect samples are granite protomylonites and mylonites hosted in the Large Pluton, where fabric ages were determined by titanite pet-

rochronology. The southern transect samples are hornblende diorite mylonites of the Misty Pluton. The detailed methods and working conditions of EBSD + CVA analyses and titanite petrochronology are summarized in the Supplemental Material¹.

RESULTS

The microstructures of the GSSZ samples from the Misty and Large Plutons show evidence of high-temperature crystal-plastic deformation (Figs. 1B and 1C). EBSD maps and photomicrographs of the microstructures are included in the Supplemental Material. In the Misty Pluton, the mylonitic fabric is defined by plagioclase and

¹Supplemental Material. EBSD methods and working conditions, sector-field LA-ICP-MS U-Pb titanite petrochronology methods, and photomicrographs and EBSD maps of the samples used for CVA analysis. Please visit https://doi.org/10.1130/GEOL.S.22280647 to access the supplemental material, and contact editing@geosociety.org with any questions.

amphibole, with plagioclase showing subgrain rotation recrystallization (SGR) microstructures indicative of dynamic recrystallization at temperatures >550°C (e.g., Passchier and Trouw, 2005), and hornblende showing undulose extinction and a strong shape preferred orientation. In the Large Pluton, the mylonitic fabric is defined by quartz, plagioclase, and biotite. Quartz is dynamically recrystallized, showing distinctive grain boundary migration (GBM) microstructures and Dauphiné twinning indicative of deformation temperatures >600°C (Barber and Wenk, 1991; Stipp et al., 2002). Plagioclase porphyroclasts show limited recrystallization and some deformation twinning, indicating temperatures above the onset of feldspar plasticity. Importantly, two out of three of the Large Pluton samples have titanite, and the titanite forms abundant clusters that are aligned with the mylonitic foliation, which we targeted for petrochronology.

Titanite petrochronology of the Large Pluton samples included imaging and mapping with

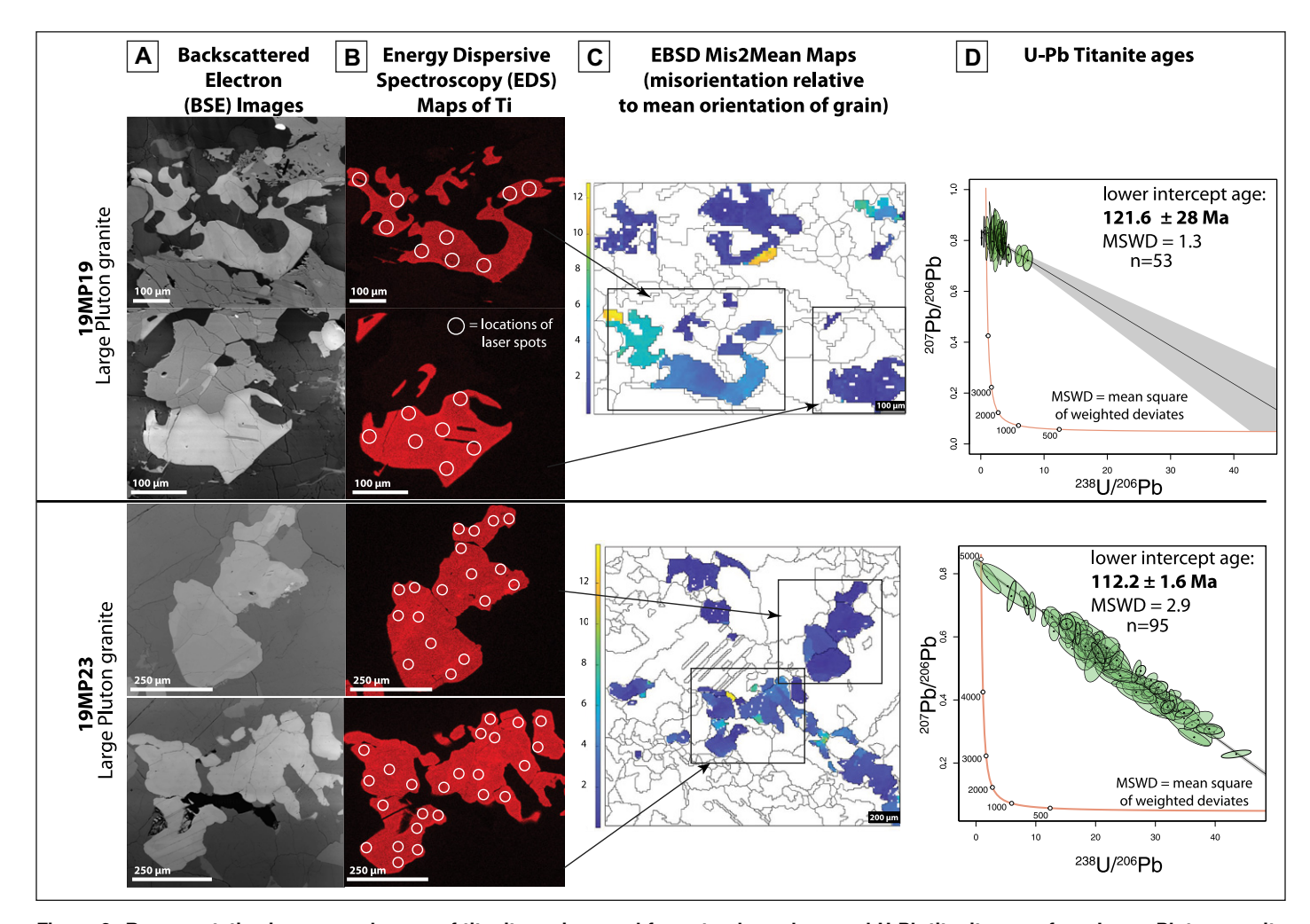


Figure 2. Representative images and maps of titanite grains used for petrochronology and U-Pb titanite ages from Large Pluton granite samples. (A) Backscattered electron (BSE) images of titanite grains. (B) Energy-dispersive spectroscopy (EDS) Ti maps of titanite grains. (C) Electron backscatter diffraction (EBSD) Mis2Mean maps showing crystal-plastic deformation in titanite grains. Color scale indicates degrees of misorientation. (D) Tera-Wasserburg concordia diagrams showing titanite data and their respective lower-intercept U-Pb age dates in two Large Pluton samples. Concordia diagrams show all spot analyses, where error ellipses are shown at 2σ .

energy-dispersive spectroscopy (EDS) and EBSD on the scanning electron microscope to confirm the metamorphic nature of the titanite grains, followed by U-Pb analysis by laser ablation-inductively coupled plasma-mass spectrometry (LA-ICP-MS) (Fig. 2). Backscattered electron images show coarse, lobate grains with slight sector zoning that correlates with the distribution of Ti, Ca, Nb, and Ce in EDS element maps (Figs. 2A and 2B; Supplemental Material). EBSD maps confirm that titanite grains display lattice bending indicative of crystal-plastic deformation (Fig. 2C). Lower-intercept ages calculated from regression of 207Pb/206Pb and ²³⁸U/²⁰⁶Pb isotope data indicate titanite growth/ recrystallization in these samples at 112 \pm 2 Ma and 122 ± 28 Ma, respectively (Fig. 2D).

CVA analysis of the Carboniferous Large Pluton and the Cretaceous Misty Pluton samples reveal important differences in kinematic deformation geometry. The titanite-bearing Large Pluton samples show that quartz and plagioclase have CVA patterns consistent with transtension, whereas the biotite and titanite CVA patterns are distinctly different and are instead consis-

В

tent with pure shear-dominated transpression (Fig. 3A). Because the titanite U-Pb ages gave a Cretaceous age of titanite growth (Fig. 2D), this demonstrates that the transpressional titanite CVA pattern (and the nearly identical biotite CVA pattern) was acquired during Cretaceous deformation of the GSSZ. Most importantly, the CVA data show that the petrochronometer (titanite) does not share the same kinematic deformation geometry as the fabric-forming quartz and plagioclase. In contrast, the Misty Pluton samples show remarkably similar CVA patterns for all fabric-forming phases, and they are all consistent with pure shear-dominated transpression (Fig. 3B), similar to the titanite and biotite CVA patterns in the Large Pluton (Fig. 3A).

DISCUSSION

In the Large Pluton, the different titanite and biotite CVA patterns relative to those of quartz and plagioclase indicate that they did not experience the same deformation history in the mylonitic fabric. This cannot be explained by strain partitioning because transpression is defined by both pure shear (compression) and simple shear components, neither of which can accommodate the tension required for transtension. Instead, the unequivocally Cretaceous age of the titanite grains demonstrates that the CVA patterns of titanite (and biotite) were acquired during the Cretaceous, during transpressional deformation. The CVA patterns of biotite are also consistent with those from a related Cretaceous transpressional intra-arc shear zone (McGinn et al., 2020). The Cretaceous age of the titanite and biotite CVA patterns implies that the quartz and plagioclase CVA patterns preserve an older, shared relict geometry. The distinctly different CVA patterns of titanite and biotite relative to quartz and plagioclase therefore demonstrate the limited utility of using titanite petrochronology to date the development of the quartz and plagioclase mylonitic fabric. If all constituent phases, including titanite, in the Large Pluton exhibited the same CVA pattern, then titanite petrochronology could be appropriately applied to date the quartz and plagioclase fabric development. By way of comparison, the similarity of CVA patterns in all the mineral phases of the

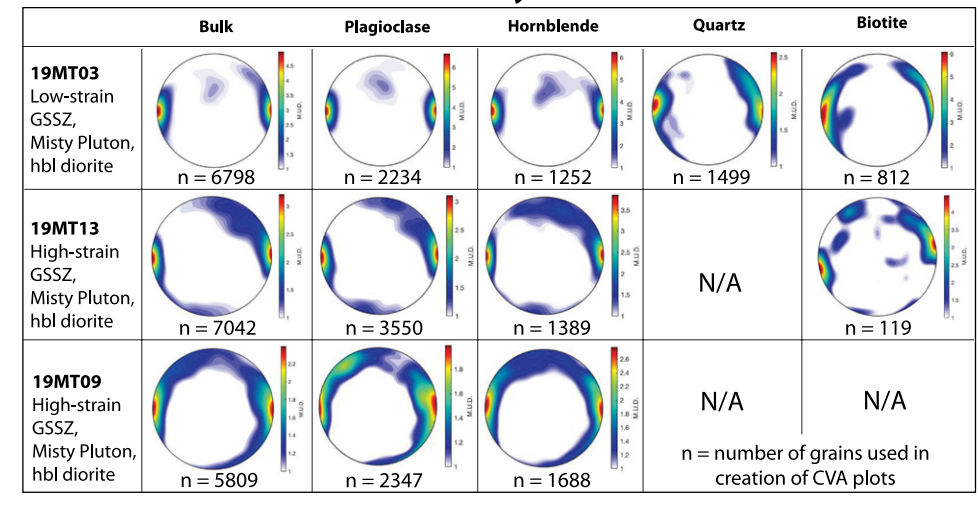


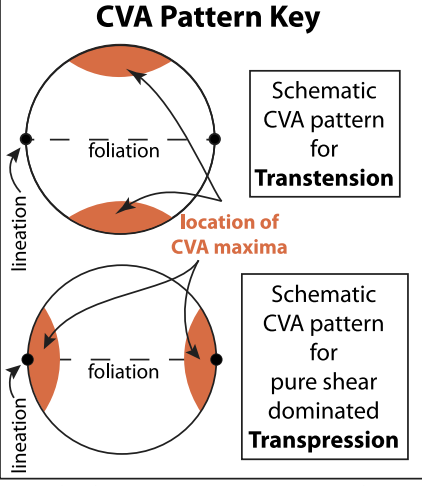
	Bulk	Plagioclase	Quartz	Biotite	Titanite
19MP19 High-strain GSSZ, Large Pluton, granite	n = 10054	n = 3317	n = 3770	n = 652	n = 19
19MP23 Large Pluton, granite	n = 14914	n = 5290	n = 5378	n = 234	n = 37

U-Pb titanite age: 121.6 +/-28 Ma

U-Pb titanite age: 112.2 +/-1.6 Ma

Cretaceous Misty Pluton CVA Data





Modified from Michels et al., 2015 and Tikoff and Greene, 1997.

Figure 3. Crystallographic vorticity axis (CVA) data for (A) Carboniferous Large Pluton granite and (B) Cretaceous Misty Pluton hornblende (hbl) diorite. CVA plots are lower-hemisphere stereographic projections and are shown in the fabric reference frame, relative to foliation and lineation. GSSZ—George Sound shear zone; M.U.D.—multiples of uniform distribution (degrees).

Cretaceous Misty Pluton demonstrates that they share the same kinematic deformation geometry and, therefore, the same fabric history.

The Carboniferous age of the Large Pluton allows for the possibility that the anomalous CVA patterns of the quartz and plagioclase were acquired during an older period of Carboniferous transtensional deformation. This implies that the quartz and plagioclase are part of a relict mylonitic fabric that was not substantially overprinted by Cretaceous deformation. Differential amounts of overprinting may also explain the slight difference in quartz/plagioclase CVA patterns between the samples. Observed field relationships are consistent with the presence of an older, relict fabric; foliation in the older interior of the Large Pluton is cut by an undeformed granitic dike with a U-Pb zircon age of 318.8 Ma (inset map in Fig. 1; Klepeis et al., 2022), suggesting a protracted period of fabric development through at least 308 Ma. An older, pre-Cretaceous fabric in the Large Pluton is best explained by its development during an older period of transtensional deformation within a shear zone along the crustal discontinuity that later became the GSSZ. A Carboniferous age of transtensional deformation is also supported by geochemical and geochronological evidence that indicates the end of the first high-MAR event was accompanied by back-arc extension in response to slab rollback and/or delamination of a mafic arc root (Turnbull et al., 2016). The extensional back-arc setting would be likely to produce Carboniferous transtensional fabrics in shear zones.

Our results show that coupled EBSD + CVA analyses are a necessary component of microstructural petrochronology and are required to date fabric development in multiply deformed shear zones. Specifically, it must be demonstrated that the CVA pattern of the petrochronometer has the same kinematic deformation geometry as that of the fabric-forming minerals targeted for dating. In the case of our samples, without individual mineral phase CVA data to accompany titanite petrochronology, the fabric in the interior of the Large Pluton would have been wrongly attributed to Cretaceous deformation. Our work also shows the power of coupled EBSD + CVA analyses in detecting cryptic, older and regional tectonic events that are otherwise hard to directly observe in the field. The exposed geology in central/western Fiordland is dominated by voluminous Early Cretaceous arc rocks of the second high-MAR event, resulting in small and discontinuous linear exposures of Carboniferous rocks from the first high-MAR event (Klepeis et al., 2022). No identifiable Carboniferous shear zones have been directly observed in these fragmented exposures, and any exposures that were present are likely to have been overprinted by the formation of the GSSZ along the linear trend of Carboniferous plutons. Despite these challenges, this microstructural technique was uniquely able to reveal evidence of a regional transtensional tectonic event, demonstrating the power of coupled EBSD + CVA in enhancing in situ petrochronology.

CONCLUSIONS

Coupled EBSD + CVA analyses combined with in situ titanite petrochronology comprise a robust tool for distinguishing overprinting relationships and dating fabrics in shear zones. We show that single-phase CVA data are needed to demonstrate that the petrochronometer and fabric-forming minerals share the same kinematic deformation geometry before in situ petrochronology can be properly applied. Our work also shows that CVA data can be combined with petrochronology to differentiate between tectonic regimes that are recorded in partially overprinted fabrics. Our results have implications for future work as well. Coupled EBSD + CVA analyses are widely applicable; they can be used on any fabrics that form above the threshold for crystal plasticity in quartzofeldspathic shear zone rocks, where common petrochronometers such as apatite (450–550°C) (Odlum et al., 2022, and references therein) and titanite (500-840°C) (Gordon et al., 2021, and references therein) have temperature sensitivities. This combined EBSD + CVA + petrochronology approach will prove to be particularly useful in the study of other long-lived shear zones where reactivation and overprinting are common.

ACKNOWLEDGMENTS

We thank Alexander Lusk, Margo Odlum, and an anonymous reviewer for constructive reviews that improved this manuscript. We thank Rose Turnbull, Richard Jongens, Harold Stowell, and Peter Lindquist for collaborative efforts in the field. We also acknowledge the assistance of Te Anau Helicopters (Te Anau, New Zealand), the New Zealand Department of Conservation, and our colleagues Andy Tulloch and Nick Mortimer at GNS Science in Dunedin. We thank Lorraine DeLao-Miranda for providing childcare during fieldwork. We thank Sabine Faulhaber at the University of California-San Diego for assistance with EBSD data collection during the pandemic. This work was supported by U.S. National Science Foundation (NSF) grant EAR-1650219 to E. Miranda, a Geological Society of America Student Research Grant to V. Brown, NSF grant EAR-40015228 to J. Schwartz, and NSF grant EAR-1119248 to K. Klepeis.

REFERENCES CITED

- Barber, D.J., and Wenk, H.R., 1991, Dauphiné twinning in deformed quartzites: Implications of an in situ TEM study of the α - β phase transformation: Physics and Chemistry of Minerals, v. 17, p. 492–502, https://doi.org/10.1007/BF00202229.
- Brown, V., 2022, Integrating Microkinematic Crystallographic Vorticity Axis (CVA) Analysis and Petrochronology to Investigate the Temporal Development of Fabric Within a Transpressional Shear Zone, New Zealand [master's thesis]: Northridge, California, California State University Northridge, 82 p.
- Buriticá, L.F., Schwartz, J.J., Klepeis, K.A., Miranda, E.A., Tulloch, A.J., Coble, M.A., and Kylander-Clark, A.R.C., 2019, Temporal and spatial varia-

- tions in magmatism and transpression in a Cretaceous arc, Median Batholith, Fiordland, New Zealand: Lithosphere, v. 11, p. 652–682, https://doi.org/10.1130/L1073.1.
- Giorgis, S., Michels, Z., Dair, L., Braudy, N., and Tikoff, B., 2017, Kinematic and vorticity analyses of the Western Idaho shear zone, USA: Lithosphere, v. 9, p. 223–234, https://doi.org/10.1130/1.518.1
- Gordon, S.M., Kirkland, C.L., Reddy, S.M., Blatchford, H.J., Whitney, D.L., Teyssier, C., Evans, N.J., and McDonald, B.J., 2021, Deformationenhanced recrystallization of titanite drives decoupling between U-Pb and trace elements: Earth and Planetary Science Letters, v. 560, https://doi .org/10.1016/j.epsl.2021.116810.
- Greenberg, G., 2022, The Importance of Amphibole in Magma Differentiation in Cordilleran Arc Crust [master's thesis]: Northridge, California, California State University Northridge, 89 p.
- Klepeis, K., Webb, L., Blatchford, H., Schwartz, J., Jongens, R., Turnbull, R., and Stowell, H., 2019, Deep slab collision during Miocene subduction causes uplift along crustal-scale reverse faults in Fiordland, New Zealand: GSA Today, v. 29, no. 9, p. 4–10, https://doi.org/10.1130/GSATG399A.1.
- Klepeis, K.A., Schwartz, J.J., Miranda, E., Lindquist, P., Jongens, R., Turnbull, R., and Stowell, H., 2022, The initiation and growth of transpressional shear zones through continental arc lithosphere, southwest New Zealand: Tectonics, v. 41, https:// doi.org/10.1029/2021TC007097.
- Kruckenberg, S.C., Michels, Z.D., and Parsons, M.M., 2019, From intracrystalline distortion to plate motion: Unifying structural, kinematic, and textural analysis in heterogeneous shear zones through crystallographic orientation-dispersion methods: Geosphere, v. 15, p. 357–381, https:// doi.org/10.1130/GES01585.1.
- Lindquist, P., 2020, The Architecture of a Lower-Crustal Shear Zone and Evidence for Along-Strike Variations in Strain Localization and Partitioning, Fiordland, New Zealand [master's thesis]: Burlington, Vermont, University of Vermont, 175 p.
- Lister, G.S., and Williams, P.F., 1979, Fabric development in shear zones: Theoretical controls and observed phenomena: Journal of Structural Geology, v. 1, p. 283–297, https://doi.org/10.1016/0191-8141(79)90003-8.
- McGinn, C., Miranda, E.A., and Hufford, L.J., 2020, The effects of quartz Dauphiné twinning on strain localization in a mid-crustal shear zone: Journal of Structural Geology, v. 134, https://doi.org/10 .1016/j.jsg.2020.103980.
- Means, W., Hobbs, B., Lister, G., and Williams, P., 1980, Vorticity and non-coaxiality in progressive deformations: Journal of Structural Geology, v. 2, p. 371–378, https://doi.org/10.1016/0191-8141(80)90024-3.
- Michels, Z.D., Tikoff, B., Kruckenberg, S.C., and Davis, J.R., 2015, Determining vorticity axes from grain-scale dispersion of crystallographic orientations: Geology, v. 43, p. 803–806, https://doi.org/10.1130/G36868.1.
- Moser, A.C., Hacker, B.R., Gehrels, G.E., Seward, G.G.E., Kylander-Clark, A.R.C., and Garber, J.M., 2022, Linking titanite U-Pb dates to coupled deformation and dissolution-reprecipitation: Contributions to Mineralogy and Petrology, v. 177, 42, https://doi.org/10.1007/s00410-022-01906-9.
- Odlum, M.L., Levy, D.A., Stockli, D.F., Stockli, L.D., and Desormeau, J.W., 2022, Deformation and metasomatism recorded by single-grain apatite petrochronology: Geology, v. 50, p. 697–703, https://doi.org/10.1130/G49809.1.

- Oriolo, S., Wemmer, K., Oyhantçabal, P., Fossen, H., Schulz, B., and Siegesmund, S., 2018, Geochronology of shear zones—A review: Earth-Science Reviews, v. 185, p. 665–683, https://doi.org/10.1016/j.earscirev.2018.07.007.
- Passchier, C.W., and Trouw, R.A.J., 2005, Microtectonics: Berlin, Springer-Verlag, 366 p., https://doi.org/10.1007/3-540-29359-0.
- Piette-Lauzière, N., Larson, K.P., Kellett, D.A., and Graziani, R., 2020, Intracrystalline vorticity record of flow kinematics during shear zone reactivation: Journal of Structural Geology, v. 140, https://doi.org/10.1016/j.jsg.2020.104134.
- Ringwood, M.F., Schwartz, J.J., Turnbull, R.E., and Tulloch, A.J., 2021, Phanerozoic record of man-

- tle-dominated arc magmatic surges in the Zealandia Cordillera: Geology, v. 49, p. 1230–1234, https://doi.org/10.1130/G48916.1.
- Stipp, M., Stünitz, H., Heilbronner, R., and Schmid, S.M., 2002, The eastern Tonale fault zone: A "natural laboratory" for crystal plastic deformation of quartz over a temperature range from 250 to 700 °C: Journal of Structural Geology, v. 24, p. 1861–1884, https://doi.org/10.1016/S0191-8141(02)00035-4.
- Tikoff, B., and Fossen, H., 1995, The limitations of three-dimensional kinematic vorticity analysis: Journal of Structural Geology, v. 17, p. 1771–1784, https://doi.org/10.1016/0191-8141(95)00069-P.
- Tikoff, B., and Greene, D., 1997, Stretching lineations in transpressional shear zones: An example from the Sierra Nevada Batholith, California: Journal of Structural Geology, v. 19, p. 29–39, https://doi.org/10.1016/S0191-8141(96)00056-9.
- Turnbull, R., Tulloch, A., Ramezani, J., and Jongens, R., 2016, Extension-facilitated pulsed S-I-A-type "flare-up" magmatism at 370 Ma along the southeast Gondwana margin in New Zealand: Insights from U-Pb geochronology and geochemistry: Geological Society of America Bulletin, v. 128, p. 1500–1520, https://doi.org/10.1130/B31426.1.

Printed in USA